CGU HS Committee on River Ice Processes and the Environment
21st Workshop on the Hydraulics of Ice Covered Rivers
Saskatoon, Saskatchewan, Canada, August 29 - September 01, 2021.

Anchor ice dam survey in small steep rivers

Einar Rødtang[1], Janik John[2], and Knut Alfredsen[3]
[1] *Department of civil and environmental engineering Norwegian University of Science and Technology 7491 Trondheim, Norway,*
einar.a.rodtang@ntnu.no

[2] *Department of civil and environmental engineering Norwegian University of Science and Technology 7491 Trondheim, Norway,*
janik.john@tuhh.de

[3] *Department of civil and environmental engineering Norwegian University of Science and Technology 7491 Trondheim, Norway,*
knut.alfredsen@ntnu.no

River ice can cause significant impact forces and damage to river infrastructure as well as ice jams and ice induced flooding. To accurately predict these phenomena, it is necessary to know the distribution of ice and ice types in a river. Steep rivers exhibit complex freeze-up behaviour combining formation of columnar ice with successions of anchor ice dams to build a complete ice cover. In these rivers, anchor ice dams can form a substantial part of the rivers volume of ice as well as be responsible for some of its thickest ice. However, little is known about how the structure of anchor ice dams varies or how to predict their locations. In this paper we describe a survey of anchor ice dams carried out during the 2020-2021 winter in the Sokna river. A tributary to the Gaula river in Middle Norway. Thin section imagery, river morphology, hydrological and meteorological data was collected. The survey uncovered substantial variation in microstructure both within and between ice dams. And a reliable statistical model for predicting the location of anchor ice dams in the studied reach was developed and evaluated.

1 Introduction

It is well known that the properties of ice vary widely. However, little is known about how the properties of anchor ice dams vary. Anchor ice dams primarily form in smaller and steeper streams in cold climates. Their formation can be described in three mayor steps. First surface water is supercooled ($T_w < 0°C$) and frazil start to develop (Stickler et al., 2010). Next the frazil ice is, trough turbulence, transported down to the river bed and accumulates, this is partly frozen to and therefore anchored to in-stream material (Lind et al., 2016). In the third step the anchor ice grows by accumulating more frazil, until it reaches the water surface causing backwater effects (Stickler et al., 2010). Because anchor ice dams can form in several locations within the river channel, this creates a step-pool morphology (Dubé et al., 2014; Stickler et al., 2010). Due to the reduction of flow velocity in these newly created pools, even steep streams can develop a complete ice cover. Turcotte (Turcotte et al., 2013) moreover describes three main stages, that an ice dam can be in. Activation: When an ice dam has just formed indicated by a rising water level and development of top ice. Passive state: When the dam has reached its final height and the water level stagnates. Breached state: When the dam becomes perforated, due to melting or mechanical fracture, and its hydraulic storage is drained. Ice dams can also be reactivated by rising water level (Turcotte et al., 2013). This can lead to further anchor ice growth or aufeis development on the dam, as well as a potentially large variety of different ice types with different material properties in the dam crest. There are several reasons why research on small streams and particularly ice dams should be encouraged:

1. Ice dams heavily influence the break-up processes in small rivers, which can in turn trigger break-ups in larger rivers causing flooding, erosion and destroying vegetation along riverbanks. Most importantly the sudden breaking of an anchor ice dam can cause a chain reaction of failing dam crests and initiate break up processes in a river, like ice runs or javes (ice jam release waves) (Rokaya et al., 2020; Turcotte et al., 2011) .
2. Conversely ice dams can also potentially hamper break up processes by stopping ice floes at their crest (Turcotte et al., 2011).
3. The total length of smaller streams is greater than the length of larger rivers, so cumulative consequences of small river and ice dam induced break up may be extensive (Lind et al., 2016).
4. Ice processes in small and steep streams differ from those in low-gradient rivers and cannot be extrapolated using research results of larger rivers (Turcotte et al., 2011).
5. Ice dams influence morphology, temperature and insulation and can therefore have implications for the in-stream flora and fauna (Dubé et al., 2014; Prowse and Culp, 2003; Stickler et al., 2010).

This paper focuses on the distribution of ice dams along the longitudinal profile of a river, as well as the distribution of ice types in ice dam crests. This was achieved by collecting GPS data of ice dam locations along a 9 km section of the river Sokna and retrieving transects of ice cores at three different ice dams and a level ice section. GIS analyses, statistical modelling, visual inspection, and thin section measurements were the main methods. The following questions shall be investigated and answered:

1. Can a statistical model including the river descriptors width, slope and sinuosity predict the locations of ice dam development?

2. What types of ice microstructure are present within an ice dam and how are they distributed?

2 Study Site

The Sokna is a small and steep river flowing through a mountainous area in central Norway. In the town Støren, which is located approximately 40 km south of the city of Trondheim, it flows into the Gaula river (see Figure 1).

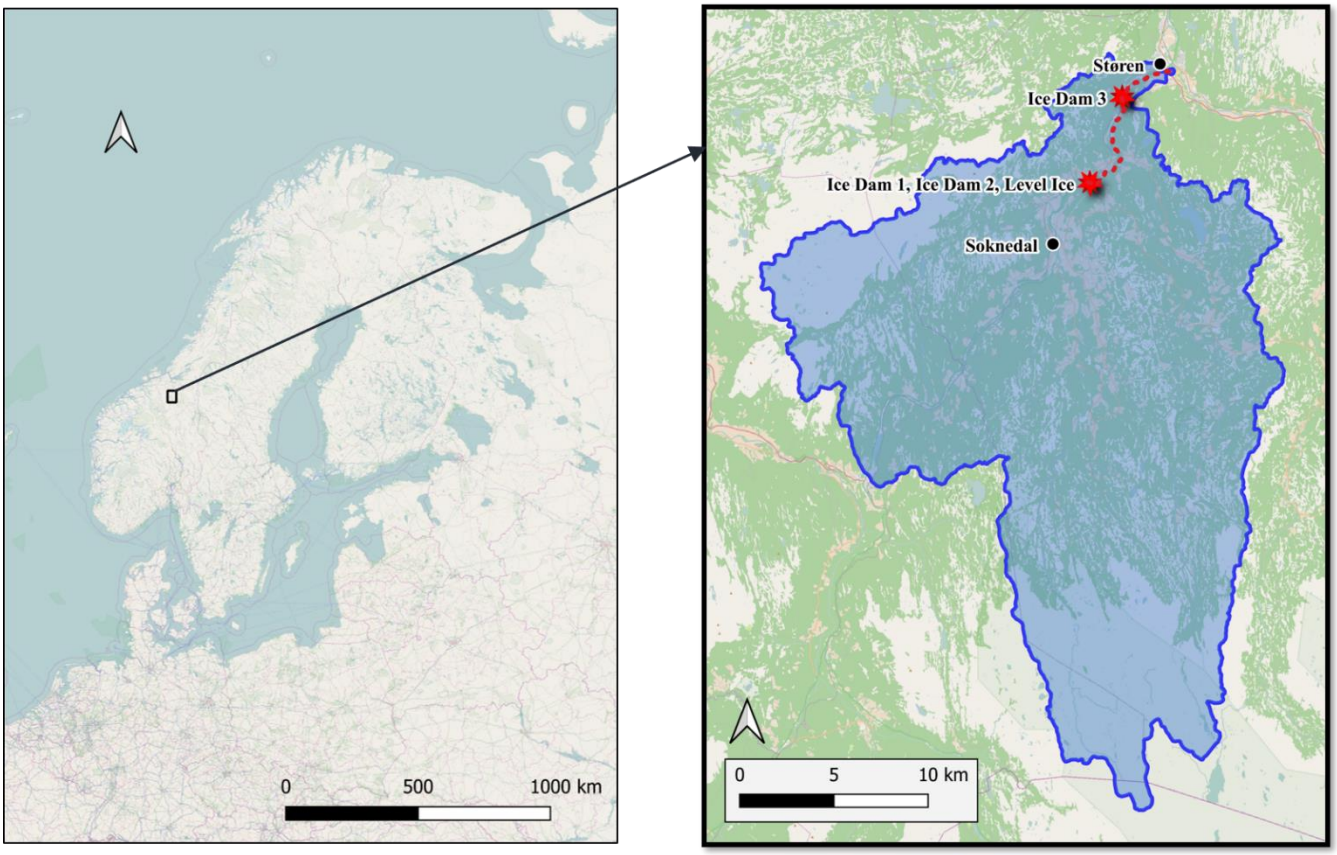

Figure 1: Location of Sokna and its catchment area

Table 1 shows a few more characteristics.

Table 1: General characteristics of the Sokna river (Stickler et al., 2010)

Catchment area	$539 km^2$
Meters above sea level	$160 m$
Mean winter flow	$2.5\, m^3/s$
Mean gradient	1.7%

The field data collection was undertaken from January 2021 until March 2021 on the lower part of the Sokna river between Soknedalstunnelen and Støren (approx. 9 km). Figure 3 shows plots of daily discharge [m³/s], precipitation [mm], mean temperature [°C], accumulated freezing degree days [°C] and snow depth [cm] for the time period between the first freezing day (20th of

October) until most snow has melted in the catchment area (30th of May). A relatively mild December with only occasional negative daily mean temperatures was followed by a cold spell starting on 30th of December and extending to 20th of January.

Figure 2: Ice Dam 1, Sokna river 5th of January 2021. Ice dam formation in progress

This cold spell initiated formation of anchor ice dams within the river, as illustrated in Figure 2. Further one should note that a dam downstream of the Hugdal Bru gauge station caused the water level to rise, which was then detected by the gauge station and falsely recorded as a rise in runoff (increase of ~900% in one week). The precipitation prior to the cold spell (~13,7 mm between 23rd and 26th of December) fell as snow and could not have produced this kind of increase. The decreasing runoff two weeks later indicates that the dam is breached, and its stored water drained.

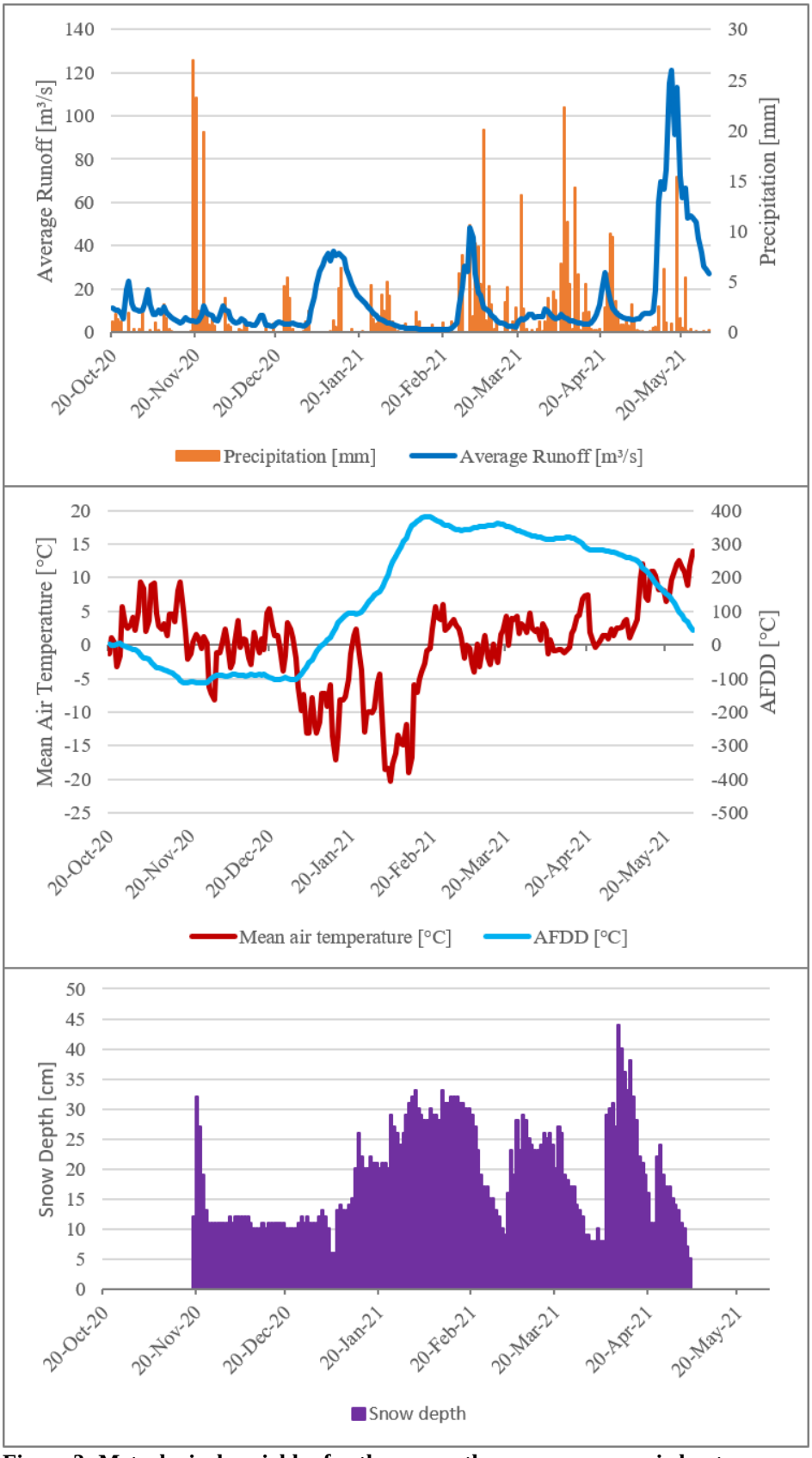

Figure 3: Metrological variables for the season the survey was carried out

3 Methodology

3.1 Ice dam location survey

To investigate how ice dams were distributed in the study area, point data was collected via GPS-measurements. This was done on four different occasions by walking and skiing on the frozen river with a GPS-stick. Only obvious ice dams were recorded (clearly visible dam crest and backwater effects (Stickler et al., 2010)). A broom was used to brush away snow and reveal the dam crest in uncertain cases. In most cases ice dams were already breached (water behind them had drained) (Turcotte et al., 2013), so clearly visible collapsed suspended ice could be used for verification. This simple method allowed counting the anchor ice dams and record their spatial distribution. The occurrence of anchor ice dams is thought to be restricted to certain areas in the river, whereas anchor ice is a phenomenon found everywhere in the river where frazil ice is produced. These “preferential zones”(Turcotte et al., 2011) contain boulders, stone clusters or large tree trunks that already block part of the cross section (Stickler et al., 2010; Turcotte et al., 2011) . Stickler (Stickler et al., 2010) also states that transition zones between fast and slow flow areas promote anchor ice dam development. To verify these observations and consider them in the spatial distribution, a digital terrain model (DTM) of the river was used and combined with the GPS data of the ice dam locations. These could then be compared to three river descriptors (width, slope and sinuosity), which were calculated at predefined data points along the rivers centreline (one point every 10 m of centreline), see Figure 4. The data processing for this was done in QGIS. To get only one value at each point along the longitudinal section of the river the centreline had to be simplified at a few locations only following the main channel of the river. Also, the width of the river had to be manually adjusted in these areas of splitting river channels. It was calculated from lines perpendicular to the centreline at each point location, that were clipped by a polygon of the water surface of Sokna. The slope was calculated along the centreline with 20 m lines having each analysed location as a midpoint. The results of four points at the bridge in Støren had to be removed as the raster values of the DTM represented the height of the bridge and not the height of the river in this area. Finally, the sinuosity was calculated choosing half a meander length (~140 m choosing the first distinct meander as reference) centred on each point. The results of the GIS processing were analysed using a binominal generalized linear model (BGLM).

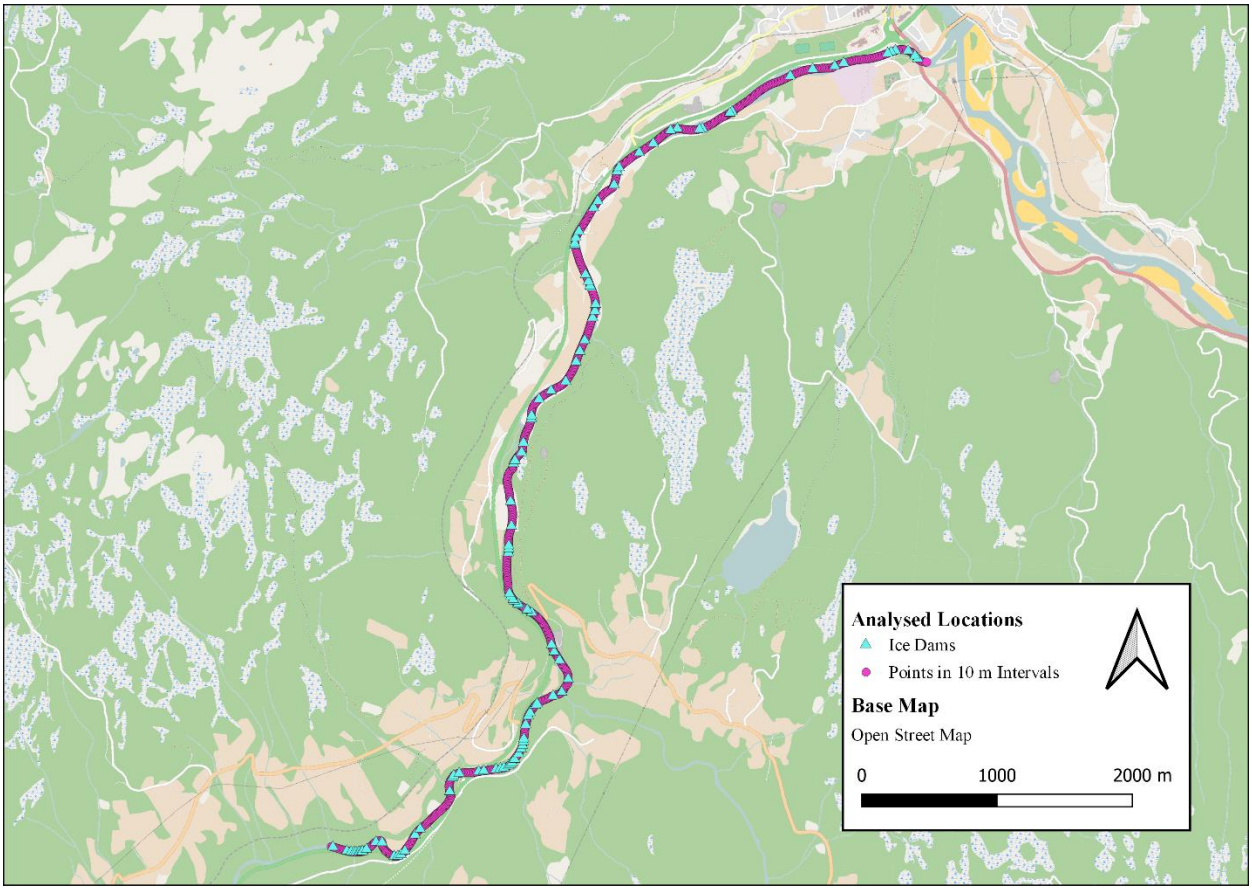

Figure 4: Analysed locations - Sokna

3.2 Thin Section lab work

For a close look at ice types and their distribution within a dam three different anchor ice dams (Ice Dam 1, Ice Dam 2, Ice Dam 3), as well as a level ice section (Level ice) were investigated more thoroughly. The snow on the dam crest was removed and ice cores were retrieved from each dam and taken into the cold lab for further investigation. Figure 5 shows a picture of Ice Core 5 of Anchor Ice Dam 3 after 2 cm thick samples were sawed out of it.

Figure 5: Ice core being processed in the lab

For each core all major ice types were identified by inspection. For each ice type identified in a core two samples were extracted, one for thin section analysis and one for density measurement (see section 4.3). The thin sections were photographed under polarized light and classified depending on type of dominant microstructure. 6 distinct types of microstructures where identified (See Table 4). Based on the findings of the lab work and ice thickness measurements drawings were created that represent the inner structure of Ice Dam 1-3 and Level ice (See Figure 9, Figure 10, Figure 11 and Figure 12).

4 Results

4.1 Ice dam location survey

Splitting the survey reach into 10m increments gives 1046 datapoints, of which 106 have associated ice dams. 7 variables were considered, river width, river slope, sinuosity, and distance along river. Whereof sinuosity was calculated in 3 different ways; fixed 140m Euclidian distance (Sinuosity140), manually variable Euclidian distance (SinusoityCustom) and Euclidian distance set by a moving window algorithm (Sinuosity_MovWin). Slope correspondingly was calculated in two ways, slope over 10m increments and slope calculated over the distances corresponding to Sinuosity_MovWin. For distributions of these variables see Figure 6.

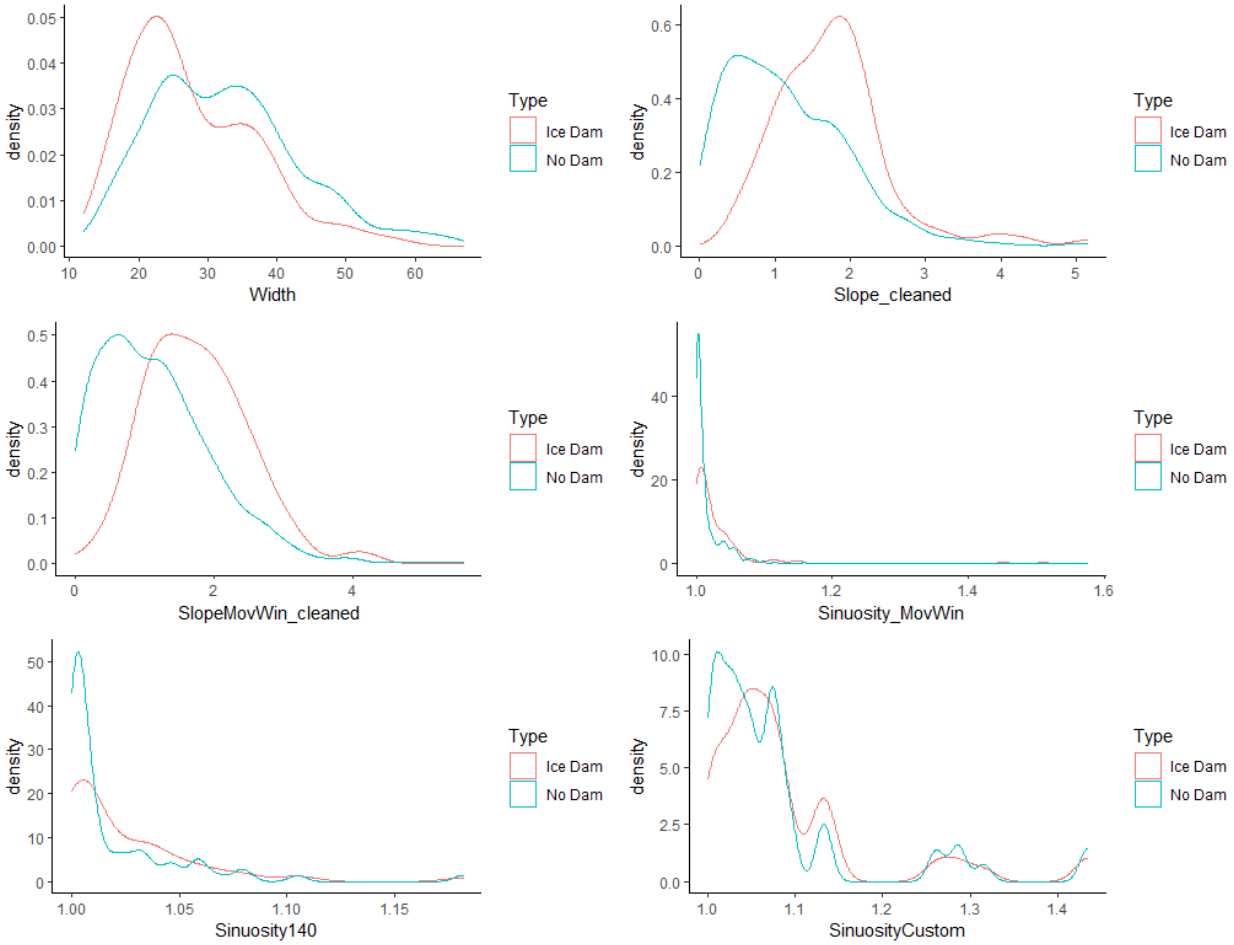

Figure 6: Density plots of ice dam survey variables

ANOVA analysis was carried out to determine which variables have significant differences in their means between the Ice Dam data points and the No Dam data points. At the 1% significance level the following variables had significantly different means between the two groups:

$$\text{Distance}\ (p = 0.00613)$$

$$\text{Width}\ (p = 1.20 \times 10^{-5})$$

$$\text{Slope\_cleaned}\ (p = 1.86 \times 10^{-12})$$

$$\text{SlopeMovWin\_cleaned}\ (p = 7.76 \times 10^{-12})$$

None of the sinuosity measures were significant:

$$\text{SinuosityMovWin}\ (\ p = 0.0703\ )$$
$$\text{Sinuosity140}\ (\ p = 0.0687\ )$$
$$\text{SinuosityCustom}\ (\ p = 0.304\ )$$

A correlation matrix was then constructed to evaluate collinearity and correlation between variables, see Figure 7. If a model has terms with too high collinearity, this is likely overfitting. If variables have very low correlation with the dependent variable, it is likely that including this variable has very low predictive power.

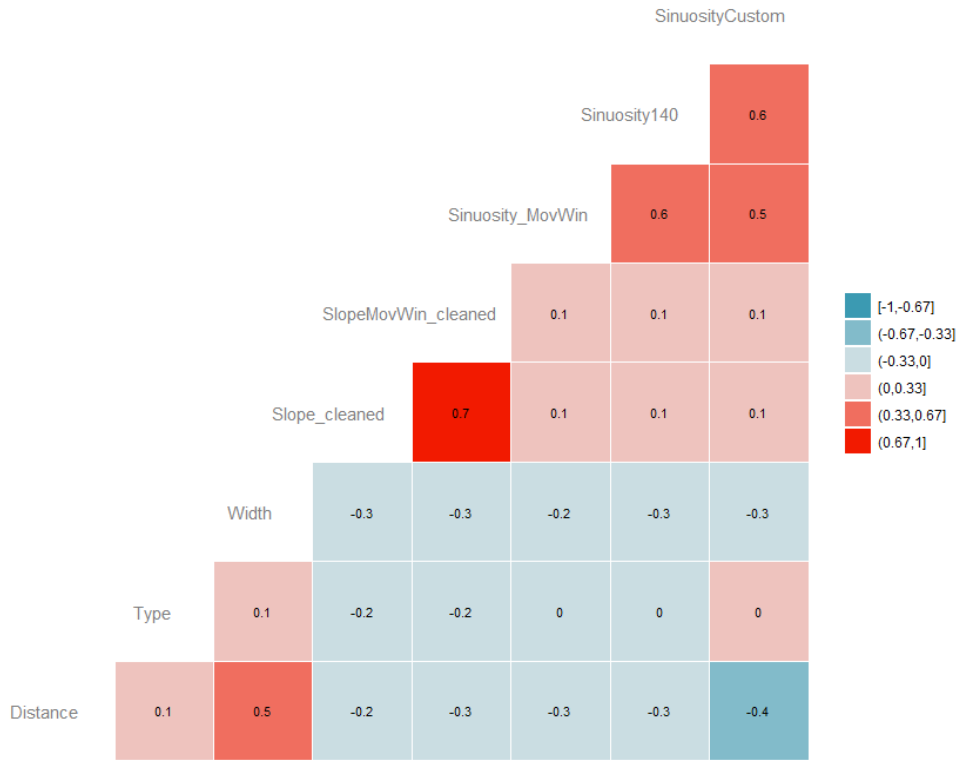

Figure 7: Correlation matrix

By physical argument, no model should contain multiple different measures for Slope or Sinuosity. Due to the very high p value of SinuosityCustom ($p = 0.304$) in the ANOVA it will not be considered further. The two measures of slope have very high collinearity (0.7), which one is chosen therefore has little importance to the performance of the model. Slope_cleaned was derived using a simpler algorithm and will therefore be used in further models. The moving window sinuosity is less prone to human bias and will therefore be preferred over the fixed distance sinuosity. Width and distance have significant collinearity; therefore, we should exclude one of them. Excluding Distance will make the model less dependent on the specific river investigated, width will therefore be included in favour of Distance.

Of these final variables (Width, Slope_cleaned and Sinuosity_MovWin) all possible combinations and two variable interactions were considered, and a corresponding binomial

generalized linear model was generated. This is summarized in Table 2. For further details on binomial generalized linear models see Gilmour (Gilmour et al., 1985).

Table 2: Model selection table, Binomial generalized linear model

	(Int)	Sns_MvW	Slp_cln	Wdt	Sns_MvW:Slp_cln	Sns_MvW:Wdt	Slp_cln:Wdt	df	logLik	AICc	delta	weight
39	1.0330		0.2168	0.07112			-0.03197	4	-316.770	641.6	0.00	0.417
40	0.9259	0.1080	0.2102	0.07104			-0.03177	5	-316.768	643.6	2.01	0.152
56	-7.4020	8.4080	0.1449	0.49820		-0.4247	-0.02929	6	-316.078	644.2	2.66	0.110
7	2.2530		-0.6120	0.02680				3	-319.488	645.0	3.42	0.075
48	1.8780	-0.7207	-0.1938	0.06796	0.3369		-0.03003	6	-316.707	645.5	3.92	0.059
64	-6.3720	7.4760	-0.1934	0.48470	0.2875	-0.4135	-0.02801	7	-316.036	646.2	4.60	0.042
24	-9.9020	11.9500	-0.6266	0.60190		-0.5660		5	-318.104	646.3	4.69	0.040
8	1.3060	0.9048	-0.6256	0.02812				4	-319.329	646.7	5.12	0.032
16	4.1410	-1.7530	-1.6770	0.02590	0.9898			5	-318.758	647.6	6.00	0.021
32	-6.1590	8.3690	-1.4800	0.52970	0.8055	-0.4964		6	-317.759	647.6	6.02	0.021
3	3.2100		-0.7214					2	-321.970	648.0	6.37	0.017
12	6.5080	-3.1650	-2.0990		1.3010			4	-320.916	649.9	8.29	0.007
4	2.9700	0.2415	-0.7262					3	-321.959	649.9	8.36	0.006
5	0.6905			0.04985				2	-332.485	669.0	27.40	0.000
22	-9.3640	9.9540		0.59790		-0.5418		4	-331.143	670.3	28.75	0.000
6	1.2730	-0.5338		0.04870				3	-332.420	670.9	29.28	0.000
2	4.5450	-2.3010						2	-341.818	687.6	46.07	0.000
1	2.1820							1	-343.103	688.2	46.63	0.000

Models ranked by AICc(x)

AICc is used to rank the models. Models with delta AICc less than 2 are considered equivalent. There is only one model with delta AICc less than 2 so we choose model 39. Notably this model does not include sinuosity.

Hence the best model is:

(1.1) $$p(icedam) = 1.0330 + 0.2168s + 0.07112w - 0.03197sw$$

Where s is slope calculated over 10m increments and w is river width.

4.2 Model performance

To estimate how good this model is it is helpful to calculate the ROC curve, see Figure 8. Note that the ideal ROC curve has an area under the curve of 1, while a fully random model would have an area under the ROC curve of 0.5. This ROC curve has an area under the curve of $0.7171618 \approx 0.72$.

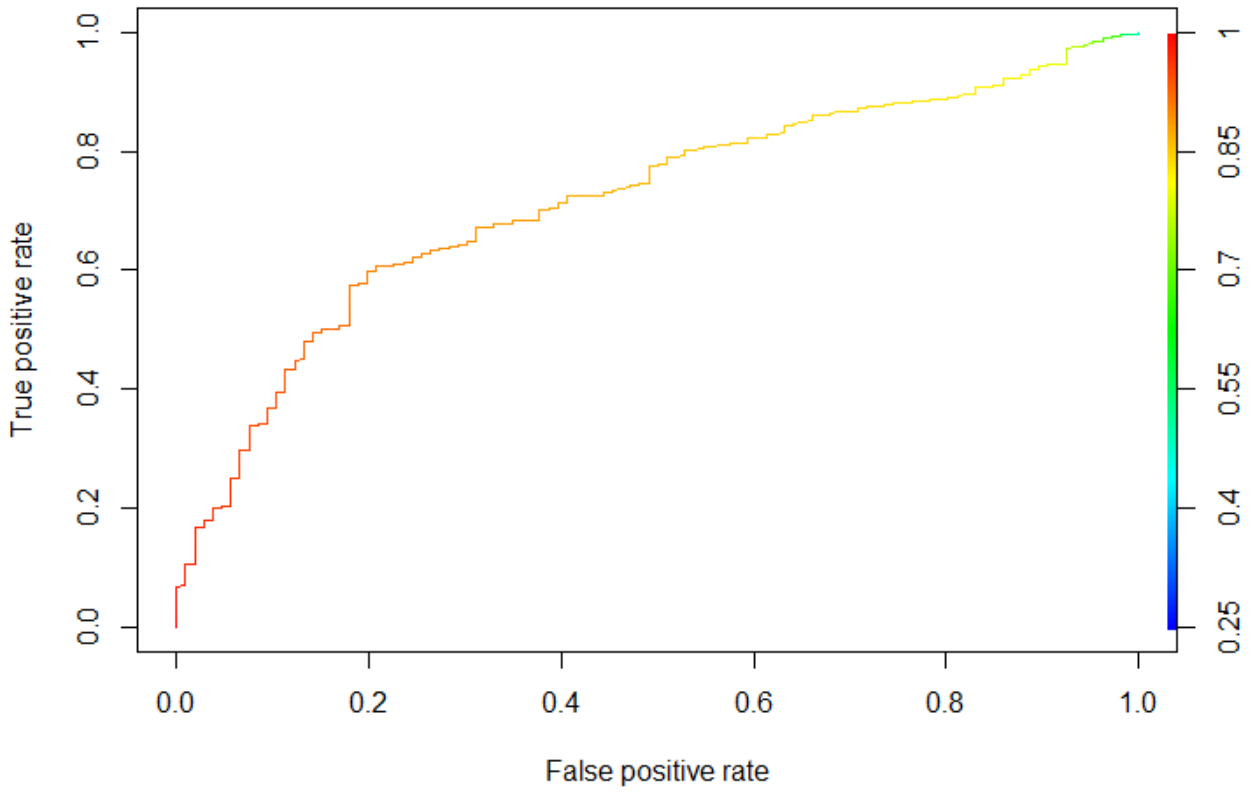

Figure 8: ROC curve

An ice dam/no ice dam cut-off probability of 0.5 results in the following confusion matrix

Table 3: Confusion matrix

	FALSE	TRUE
Ice Dam	0	106
No Dam	2	938

The confusion matrixes low false positive and false negative gives us some confidence in our model. It does not exclude the possibility of overfitting, however our model has relatively few parameters compared to data points. Carrying out "Leave One Out Cross Validation" (LOOCV) using this model and the full data set results in a prediction error of 0.103250 ≈ 0.1. The cross validation was carried out using the cv.glm() function in the boot package. Setting the cost function as suggested by the cv.glm() documentation for binomial glms. To see the data and complete R Code used to conduct this statistical analysis see:

https://github.com/ERodtang/Anchor_ice_dam_survey

4.3 Ice dam microstructure survey

A total of 72 thin sections where made and photographed under polarized light. These were cut from 27 ice cores divided among 3 ice dam transects and 1 level ice transect. These thin sections were classified according to similarity to each other. This resulted in 6 distinct classes, labelled A-F. Table 4 contains an overview of these microstructures.

Table 4: Representative thin section images

A – Ice Dam 2, Core 3, 4cm from top	B – Ice Dam 1, Core 8, 17cm from top

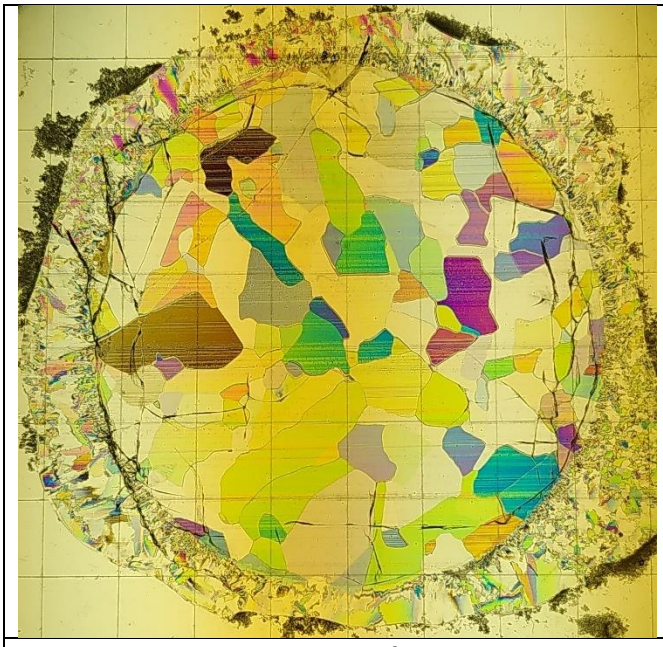	
C – Level ice, Core 1, 30cm from top	D – Ice Dam 2, Core 5, 60cm from top
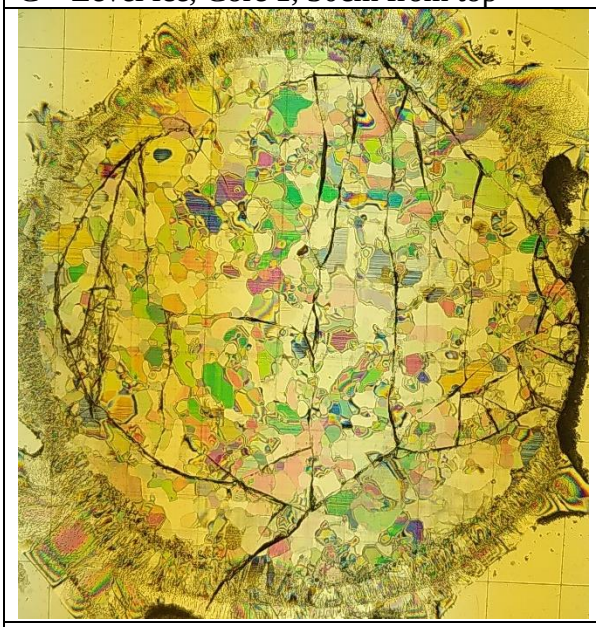	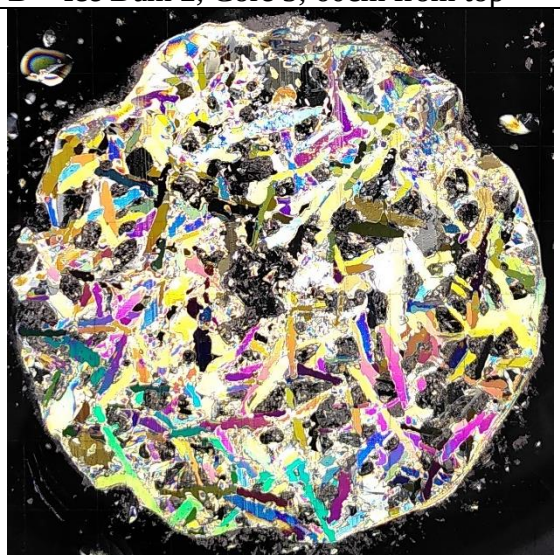
E – Ice Dam 1, Core 6, 77cm from top	F – Ice Dam 3, Core 1, 8cm from top

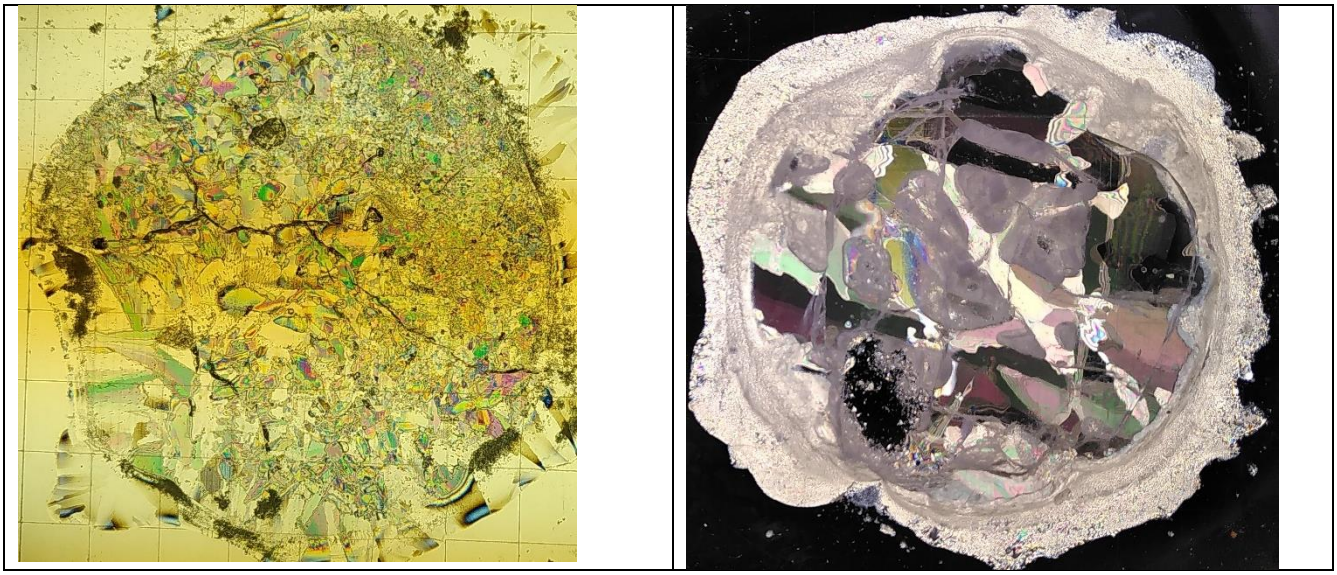

Of these microstructures 19 were type A, 11 were type B, 7 Type C, 8 type D, 21 Type E and 1 type F. Thin section microstructures were not always amenable to this classifications system and would frequently fall ambiguously between categories. The two primary categories were needle structure and non-needle structure (A,C,E,F=Non-needle structure and B,D=Needle-structure). Minor variation in thin section thickness, camera settings and melt damage to the cores made analysing the thin sections more difficult.

Figure 9 - Figure 12 shows height of and distance between retrieved ice cores. As well estimated regions of similar microstructure. Note that grain size in particular changes continuously with height, so transition between zones is often diffuse. Cores marked “Unknown” were lost before analysis was possible due to a faulty freezer. Some of the key takeaways for the level ice are: The Level ice does not contain needle-structure type ice and the larger grained type “A” ice tends to not form directly at the surface. This is consistent with rapid growth at the surface due to little insulation from overlying ice and generally slower growth further down as the insulation from overlying ice increases.

Trends are more difficult to glean from the ice dam figures. Dominant ice type within dams is not necessarily consistent between dams. The top of the ice dam often consists of Type “A” ice. Which is consistent with top ice growing upwards when water overflows the crest. While the cores collected were generally taken from the thickest parts of the ice dam it is worth pointing out that drained ice dams frequently contain large voids and successive suspended layers of thin ice.

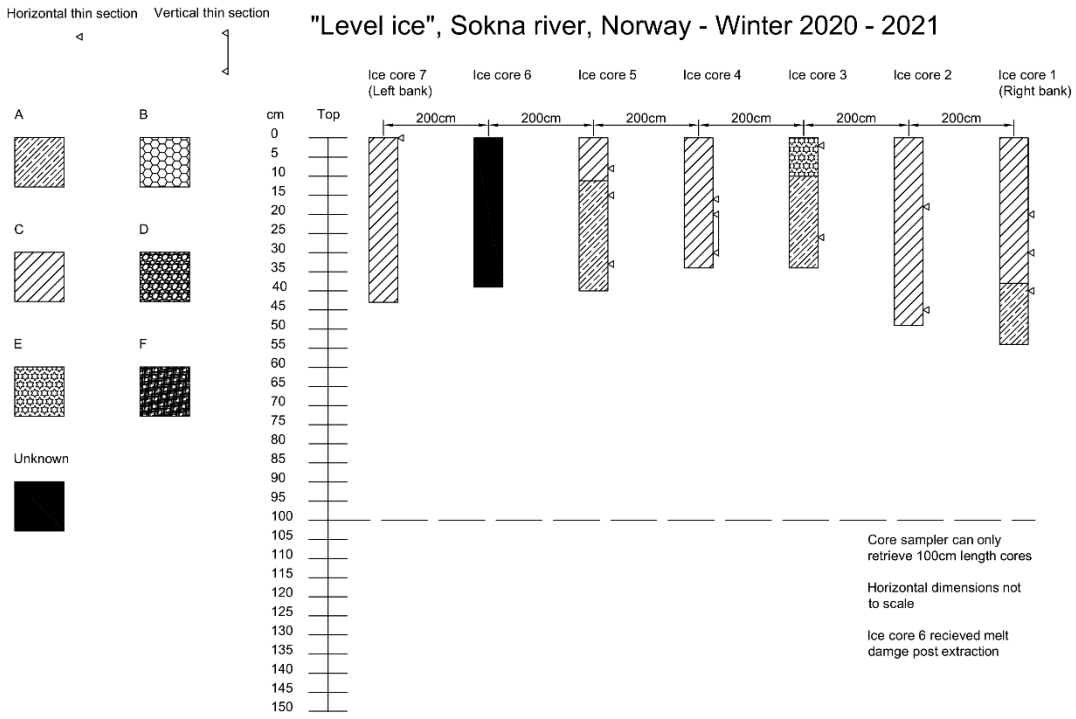

Figure 9: "Level ice", Sokna River, Norway - Winter 2020 - 2021

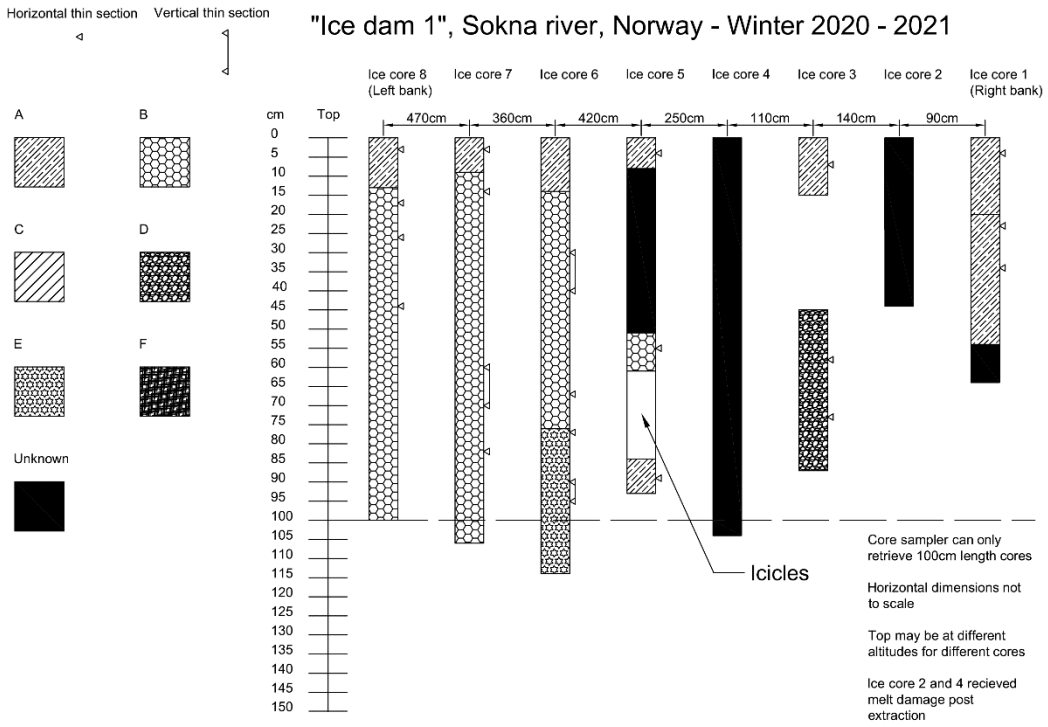

Figure 10: "Ice dam 1", Sokna River, Norway - Winter 2020 - 2021

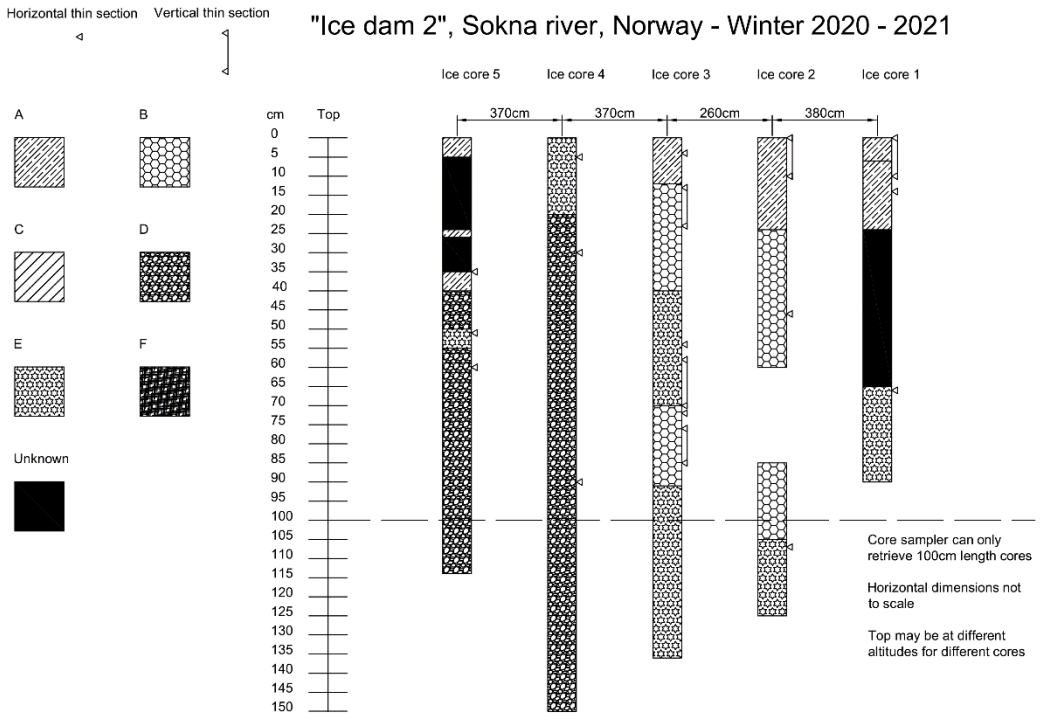

Figure 11: "Ice dam 2", Sokna River, Norway - Winter 2020 - 2021

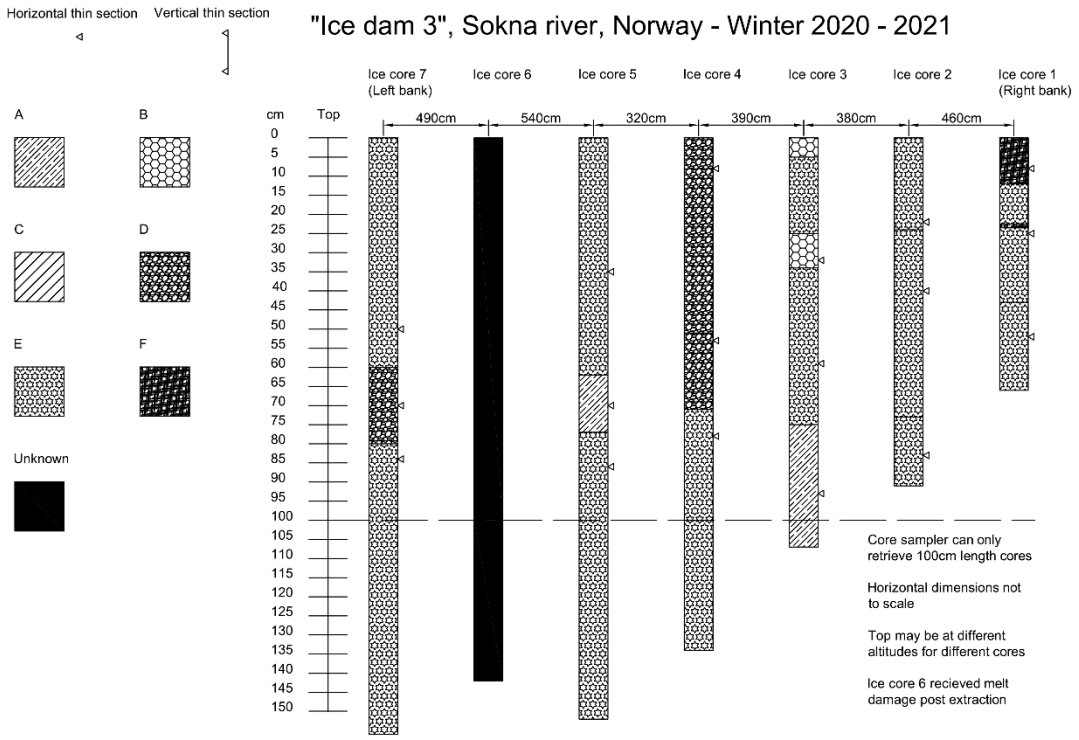

Figure 12: "Ice dam 3", Sokna River, Norway - Winter 2020 - 2021

5 Discussion

5.1 Ice dam microstructure survey

While the distribution of ice within an ice dam can justifiably be referred to as chaotic, some useful observations can be gleaned from the thin section survey. Much of the variability can be traced back to the number of different ice growth mechanism work in an ice dam. Whereof the primary ones are:

Top ice growth:
Occurs when high discharge or inability of flow to penetrate through the ice dam causes water to flow over the crest of the ice dam. Grain size will depend on water temperature, air temperature and height of water column above the ice dam crest. This ice type is like aufeis and will have a rice-paddy like macrostructure.

Columnar/Pseudo-columnar ice growth:
Occurs when the ice cover thermally grows downwards. Turbulence and water-level changes may disrupt columnar growth and as such fully columnar growth usually doesn't last long in anchor ice dams. The characteristic microstructure for microstructure A is distinctly columnar. Usually however the microstructure is less pure and looks closer to microstructure C.

Snow ice:

Occurs when accumulated snow on the top of the ice cover is flooded and then freezes. This papers data set does not contain snow ice because once snow deposited on the ice dams, the dams were already breached, and discharge did not increase sufficiently to generate snow ice.

Icicle growth:
Icicles and similar structures grow through atmospheric heat diffusion and thin film fluid mechanics (Short et al., 2006). During the survey ice dams were observed to often have substantial volumes of icicles on their downstream side.

Anchor ice growth:
Anchor ice grows from the riverbed and up due to frazil deposition and in-situ growth (Ghobrial and Loewen, 2021). Anchor ice often forms during the night and releases during the day due to insolation. In Sokna the steep valley causes there to be little insolation and anchor ice release is consequently rare.

Which mechanism is dominant at any given point in an ice dam at any given time depends heavily on the growth history of the dam as well as current temperature, discharge and frazil flow rate.

5.2 Ice dam model evaluation

6 Conclusion

Anchor ice dams have microstructure that varies significantly within and between ice dams and are generated by a variety of mechanisms.

In the reach studied for the year studied the model:

(1.2) $$p(icedam) = 1.0330 + 0.2168s + 0.07112w - 0.03197sw$$

Where s is river slope and w is river width, describes the probability of finding an ice dam at a given location rather well. To determine the general applicability of this model it will be necessary to test it against data for other rivers as well as data from the same river but from a different year. For the river studied this model achieves an ROC area under the curve of approximately 0.72. Leave one out cross validation of this model gives a prediction error of approximately 0.1

The anchor ice dam location data from Sokna and subsequent statistical analysis implies that the measures of sinuosity considered are poor predictors of anchor ice dam location in Sokna. To confidently generalize this conclusion, it will be necessary test this hypothesis against data from other rivers with higher sinuosities. It is worth investigating whether other measures of river sinuosity, such as local curvature, have predictive power.

Of the ice generated in Sokna (Average slope 1.7%) approximately 10% by river length was part of anchor ice dams. Anchor ice dam sections were observed to have 2-3 times thicker ice than nearby level ice sections, hence an estimated 20% of the ice volume of Sokna was part of anchor ice dams. Therefore, furthering our understanding of anchor ice dams is critical for understanding ice dynamics in steep rivers.

7 Funding

Norwegian University of Science and Technology (NTNU)

8 Acknowledgements

Vegard Hornes for help gathering data.

9 References

Dubé, M., Turcotte, B., Morse, B., 2014. Cold Regions Science and Technology Inner structure of anchor ice and ice dams in steep channels. Cold Reg. Sci. Technol. 106–107, 194–206. https://doi.org/10.1016/j.coldregions.2014.06.013

Ghobrial, T.R., Loewen, M.R., 2021. Continuous in situ measurements of anchor ice formation, growth, and release. Cryosphere 15, 49–67. https://doi.org/10.5194/tc-15-49-2021

Gilmour, A.R., Anderson, R.D., Rae, A.L., 1985. The Analysis of Binomial Data by a Generalized Linear Mixed Model. Biometrika 72, 593–599.

Lind, L., Alfredsen, K., Kuglerová, L., Nilsson, C., 2016. Hydrological and thermal controls of ice formation in 25 boreal stream reaches. J. Hydrol. 540, 797–811. https://doi.org/10.1016/j.jhydrol.2016.06.053

Prowse, T.D., Culp, J.M., 2003. Ice breakup: A neglected factor in river ecology. Can. J. Civ. Eng. 30, 128–144. https://doi.org/10.1139/l02-040

Rokaya, P., Morales-Marin, L., Lindenschmidt, K.-E., 2020. A physically-based modelling framework for operational forecasting of river ice breakup. Adv. Water Resour. 139, 103554. https://doi.org/10.1016/j.advwatres.2020.103554

Short, M.B., Baygents, J.C., Goldstein, R.E., 2006. A free-boundary theory for the shape of the ideal dripping icicle. Phys. Fluids 18. https://doi.org/10.1063/1.2335152

Stickler, M., Alfredsen, K.T., Linnansaari, T., Fjeldstad, H.-P., 2010. The influence of dynamic ice formation on hydraulic heterogeneity in steep streams. River Res. Appl. 26, 1187–1197. https://doi.org/10.1002/rra.1331

Turcotte, B., Morse, B., Anctil, F., 2011. Steep channels freezeup processes. CRIPE 85–101.

Turcotte, B., Morse, B., Dubé, M., Anctil, F., 2013. Quantifying steep channel freezeup processes. Cold Reg. Sci. Technol. 94, 21–36. https://doi.org/10.1016/j.coldregions.2013.06.003